

CHRISTOPHER NEWPORT UNIVERSITY

---

# GATE Simulation for the RDG PhytoPET System

---

*Author:*

Carly WEVER

*Supervisor:*

Dr. Peter MONAGHAN

April 24, 2020



# Contents

<b>Abstract</b>	<b>2</b>
<b>Acknowledgements</b>	<b>3</b>
<b>Introduction</b>	<b>4</b>
<b>Theory</b>	<b>5</b>
<b>Methods</b>	<b>8</b>
mainRDG.mac . . . . .	9
visuRDG.mac . . . . .	9
verboseRDG.mac . . . . .	10
worldRDG.mac . . . . .	10
geoRDG.mac . . . . .	12
source_2gammasRDG.mac . . . . .	16
physicsRDG.mac . . . . .	17
petDigiRDG.mac . . . . .	18
outputRDG.mac . . . . .	21
<b>Data</b>	<b>22</b>
<b>Discussion</b>	<b>26</b>
<b>Appendix</b>	<b>28</b>
Appendix A . . . . .	29
Appendix B . . . . .	29
Appendix C . . . . .	30
<b>References</b>	<b>33</b>

# Abstract

The Radiation Detector & Imaging Group (RDG) at Thomas Jefferson National Accelerator Facility (JLab) provides nuclear physics detector expertise and engages in technology transfer of its research to facilitate the development of medical applications and plant biology research. One of the projects the RDG is working on is called phytoPET: a plant imaging Positron-Emission Tomography (PET) system in which RDG detectors surround a plant that is given a radioactive tracer in order to render a 2D image that can help researchers better understand carbon transport and plant productivity. The primary type of detector developed for this purpose consists of scintillators and position sensitive photomultiplier tubes (PSPMTs) to detect radiation from sources such as plants or rats. At present, the RDG's Research and Development (R&D) process consists of physically building a detector based on the team's conglomerate experience and current research in available literature. The RDG wished to incorporate GEANT4 Application for Emission Tomography (GATE), a software tool designed to model and simulate experiments pertaining to nuclear medicine, into their R&D process. The primary purpose of this project was to simulate a simplified configuration for the well-known phytoPET system in GATE to verify its results with available experimental data. Through this project, GATE was determined a suitable tool for the RDG to employ in their research and design of future detector systems. The GATE macros and Python code written for this project will serve as a template for the RDG to further model components of their detector system. This project helped initiate the integration of GATE into the RDG's R&D process in order to analyze designs and evaluate results in a more cost-effective and innovative way.

## Acknowledgements

I would like to express my deep gratitude to Dr. Peter Monaghan, my research advisor, for his guidance and encouragement during this project. I would also like to thank Dr. Drew Wisenberger and the other members of the Radiation Detector and Imaging group at Jefferson Labs for this research opportunity and their support. My grateful thanks are also extended to Dr. Brad Sawatzky for his help in installing GATE and setting up a Jupyter Notebook Kernel at Jefferson Labs.

# Introduction

The Thomas Jefferson National Accelerator Facility (JLab) is a United States Department of Energy (DOE) national laboratory studying fundamental nuclear physics. The lab consists of an electron accelerator and four experimental halls. By scattering electrons from fixed targets, the structure of neutrons and protons and the interactions of their building blocks are explored. The Radiation Detector & Imaging Group (RDG) at JLab provides nuclear physics detector expertise to facilitate the nuclear physics research program at JLab. Additionally, the group engages in technology transfer of its research to facilitate the development of medical applications and plant biology research. The primary type of detector developed for this purpose are scintillator-based detectors. These use a combination of scintillators and position sensitive photomultiplier tubes (PSPMTs) to detect radiation from sources such as plants or rats. These types of detectors are utilized in Positron-Emission Tomography (PET) imaging, a technology in medicine used to develop 2D and 3D images of a patient's organs. The patient is injected with a radioactive tracer, which produces radioactivity in the organ. The image of the organ is formed by detecting the radiation emitted using a scintillator based detector system.

PhytoPET is a plant imaging PET system designed and built by the RDG and comprised of two detector modules with a radiation source in between them [1]. My project modeled a simplified version of the phytoPET system using GEANT4 Application for Emission Tomography (GATE), a software tool designed to model and simulate experiments pertaining to nuclear medicine such as medical imaging and radiotherapy [2]. At present, the RDG's Research and Development (R&D) process consists of physically building a detector based on the team's conglomerate experience and current research in available literature. The RDG wanted to incorporate GATE into their R&D process to analyze their designs and evaluate their results. The group is specifically interested in GATE because it has the flexibility to

design and simulate PET detectors that do not pertain solely to medical operations, such as phytoPET. The ultimate goal was to model a well known, working detector the group has built. Simplified experiments with a virtually-built phytoPET system in GATE were simulated. Using Python, the simulated data was compared with the RDG’s available experimental data.

## Theory

The antiparticle of an electron, the positron, was first discovered by C.D. Anderson in 1932 [3]. In Positron Emission Tomography (PET) scanning, a patient is injected with a positron-emitting radioactive chemical (e.g. Carbon-11 or Fluorine-18). This chemical will mainly congregate in cancerous cells and produce a positron ( $e^+$ ). The positron emitted from a radioactive nucleus travels for a short period of time before it loses the majority of its kinetic energy through atomic collisions and is attracted to an electron.

The electron and positron orbit around one another (creating the “atom” positronium) and annihilate one another in approximately  $10^{-10}$  seconds [3]. This annihilation producing electromagnetic (EM) radiation can be denoted:

$$e^+ + e^- = \gamma + \gamma \tag{1}$$

Typically, two gamma photons are produced in order to conserve energy,

$$2m_e c^2 \approx h\nu_1 + h\nu_2 \tag{2}$$

where  $\nu_1$  and  $\nu_2$  are the respective frequencies of each photon produced,  $c$  is the speed of light, and  $m_e$  denotes the mass of an electron. This is an approximation because the atomic binding energy is not incorporated into the equation. In the center of mass frame of the

annihilating  $e^+e^-$  pair, the total momentum will be zero and, by momentum conservation, is shared between the two photons and so,

$$0 = \frac{h\nu_1}{c} - \frac{h\nu_2}{c} \quad (3)$$

Since the photons are massless, they have no rest mass energy and consequently all of the available energy in the annihilation is transformed into kinetic energy of the two photons. So by equation (3),  $\nu_1 = \nu_2 = \nu$  and therefore by energy conservation,

$$2m_e c^2 = 2h\nu = 1.022 \text{ MeV} \quad (4)$$

The two photons emitted from the annihilation will travel in opposite directions with the same energy of 0.511 MeV.

Tumors in a patient can be located by measuring the direction of the gamma ray photons (at the right energy level of 0.511 MeV) detected in coincidence [3]. This is called the Line of Response (LOR) method. Figure 1 illustrates how this works.

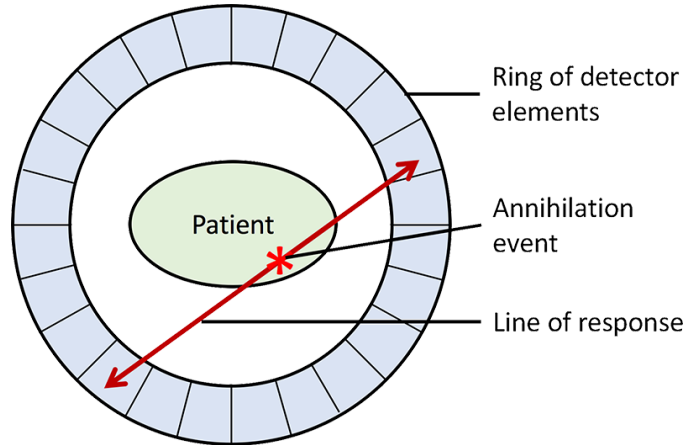
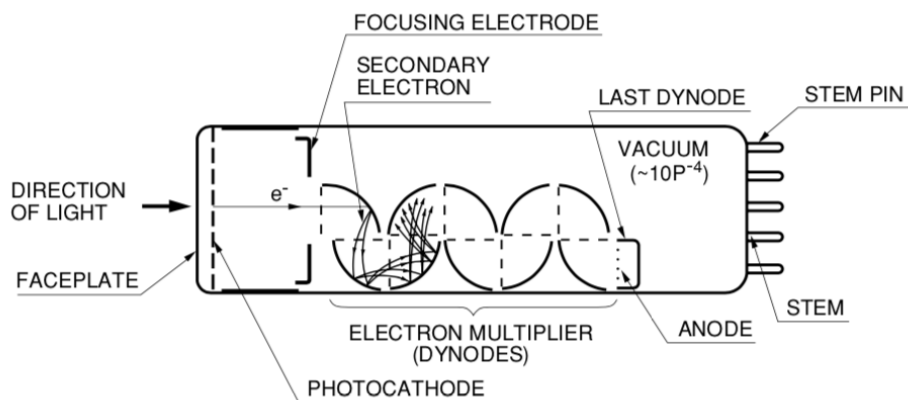


Figure 1: Illustration of the photon emission process from the annihilation of an electron-positron pair [4]

One of the RDG experiments involves exposing a plant to positron emitting  $^{11}\text{CO}_2$  in

an “environmental growth chamber” [1]. PET imaging of a plant using  $^{11}\text{CO}_2$  can help researchers study carbon transport and bio-efficiency within plants [5]. The detectors modeled in GATE are used to identify and record these gamma ray photons as electrical signals. The  $\gamma$ -ray first passes through a one-mm thick,  $48 \times 48$  array of scintillators [6] made of LSO crystal [1]. The scintillator absorbs a fraction of the ionizing radiation and converts some of this energy into either ultraviolet (UV) or visible light [7]. Next, the photon passes through a three-mm thick light guide, then through the glass face of the position sensitive photomultiplier tube (PSPMT), and hits the photocathode which is on the inner surface of the glass face [1]. These PSPMTs are specifically designed with an  $8 \times 8$  matrix of anodes so “crosstalk” can occur. This crosstalk measures the accuracy of the signal incident at a position of the photocathode detected while still retaining position information [8]. Therefore, crosstalk is crucial to tracing back where the event hit the crystal matrix. This collision knocks off a primary electron that then strikes the first dynode of a chain of dynodes. This first hit emits a number of secondary electrons (see Figure 2 below). This group of secondary electrons hits another dynode surface, producing more secondary electrons. This process continues along the whole dynode chain resulting in an amplification of the original electron charge [8]. By the end of the dynode chain, an  $8 \times 8$  matrix of anodes collects the cascade of electrons and outputs an electron current to a four channel readout [1] so as “to simplify readout electronics” [9].





THBV3\_0201EA

Figure 2: Diagram of a typical PMT [10]

These are the physical processes that occur to then create a 2D or 3D image of the region of interest (ROI) that is emitting the radioactive chemical. The phytoPET system produces 2D images that reveal the distribution and utilization of carbon dioxide ( $\text{CO}_2$ ) in the plant as shown below:

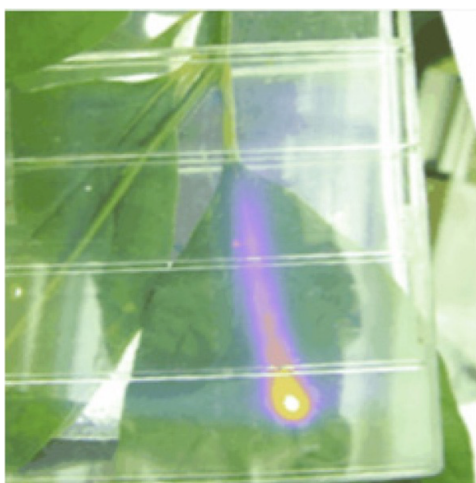


Figure 3: Photo of leaf with image of Carbon-11 distribution overlaid [5]

## Methods

The RDG purchased a computer dedicated to running GATE. After it was delivered in October 2019, GATE V8.2 was installed with all of its dependencies. After installing GATE, benchmark tests were run in order to validate the installation. Only one of the seven tests (benchImaging.optical) passed. Most likely, the other six failed because those tests were created before the more current versions of GATE and its dependencies were published.

One of the software developers, David Sarrut, created a folder of example macros and Python code (for data analysis) with brief instructions of the expected output of these programs [11, 12]. These examples were downloaded and worked through as a substitute to test if GATE was installed correctly on the RDG computer. The example macros produced the expected results and could be plotted with Jupyter Notebooks. One of the folders in Sarrut’s “gate-exercices” was a PET simulation. This folder of macros was used as a starting point for the phytoPET simulation.

The particular design and setup of the simulation geometry were chosen to mimic the actual RDG phytoPET system as closely as possible. The phytoPET simulation has a total of nine macros: mainRDG, visuRDG, verboseRDG, worldRDG, geoRDG, source\_2gammasRDG, physicsRDG, petDigiRDG, and outputRDG. All of these macros and folders are uploaded to a GitHub account (<https://github.com/cmwever/phytoPET>).

### **mainRDG.mac**

Each of the other nine macros are called in the Main macro to initialize and run the GATE simulation. The Main macro also sets the simulation’s runtime (see Appendix A). GATE uses Monte Carlo simulations, so a random number generator and its seed is defined in this macro.

## **visuRDG.mac**

This macro is called first in the main macro to open a Graphical User Interface (GUI), in which parts of the simulation that have visual components can be ‘drawn’ as the simulation runs. In this case, Open Graphics Library Immediate Qt (OGLIQt) is opened, axes are specified, trajectories are drawn in real time as particles travel within the World, and the vantage point at which the GUI will display can be set. For this project 40 cm arrows are drawn (and labeled) at 90° to represent the X, Y, and Z axes. The display for the trajectories of the  $\gamma$ -rays were enabled as a validation that the radiation was emitted from the source at specified angles (see source\_2gammasRDG.mac).

## **verboseRDG.mac**

The verbosity of different elements of the simulation are set here. This macro essentially sets how many (if any) print statements are generated about the status of a simulation as it runs. Each element can be assigned a 0, 1, or 2. Each number, respectively, increases the verbosity of the simulation. For phytoPET, this macro has all aspects of the simulation set to 0 to save memory and reduce simulation time. If trouble-shooting is necessary, the values could be increased to then read what specific elements of the simulation are producing problems.

## **worldRDG.mac**

The world macro sets up the 3-dimensional space that contains the entire simulation. For this particular project, the World is set to be 50 cm<sup>3</sup>. The outline of this cube is colored White and is filled with Air (a pre-made compound in GateMaterials.db). This macro also calls the Gate Materials database so it can be referenced in other macros. In addition, GATE has a Materials.xml file which contains materials (e.g. Liver, LSO, Water) that are

made from the elements listed in the GateMaterials database. The Materials.xml did not originally contain Lutetium Yttrium Orthosilicate (LYSO) crystal. It was added to the list by referencing two papers [13, 14] to obtain the values needed to create the new material.

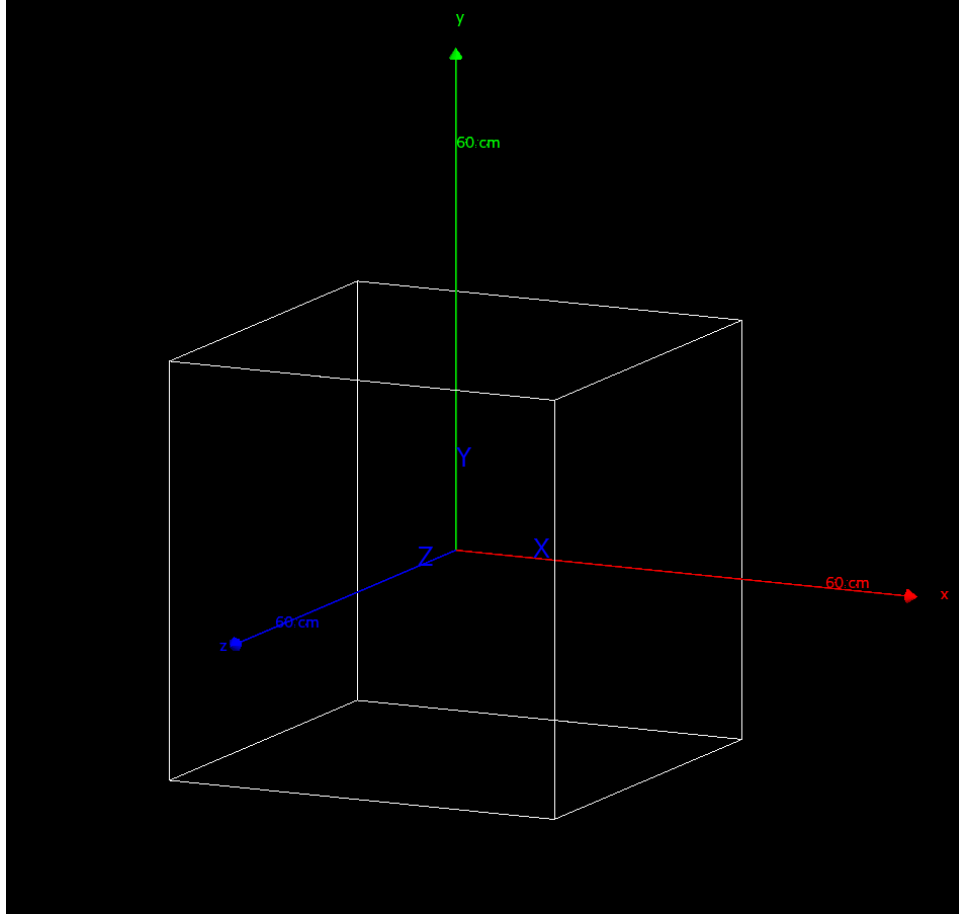


Figure 4: World with Axes in OGLIQt GUI

## geoRDG.mac

Of the predefined systems in GATE, the Ecat system most closely resembles the setup that phytoPET requires which consists of three levels within the World. The first is the Base which is in the shape of a ring. The cylinder (ring) is set to have an inner radius of 14 cm, an outer radius of 16 cm, and a height of 5 cm. These dimensions are predicated on the RDG's physical configurations with the detectors 30 cm apart and the 1.0 cm thick array of scintillating crystal. Figures 5 & 6 shows the Base configuration:

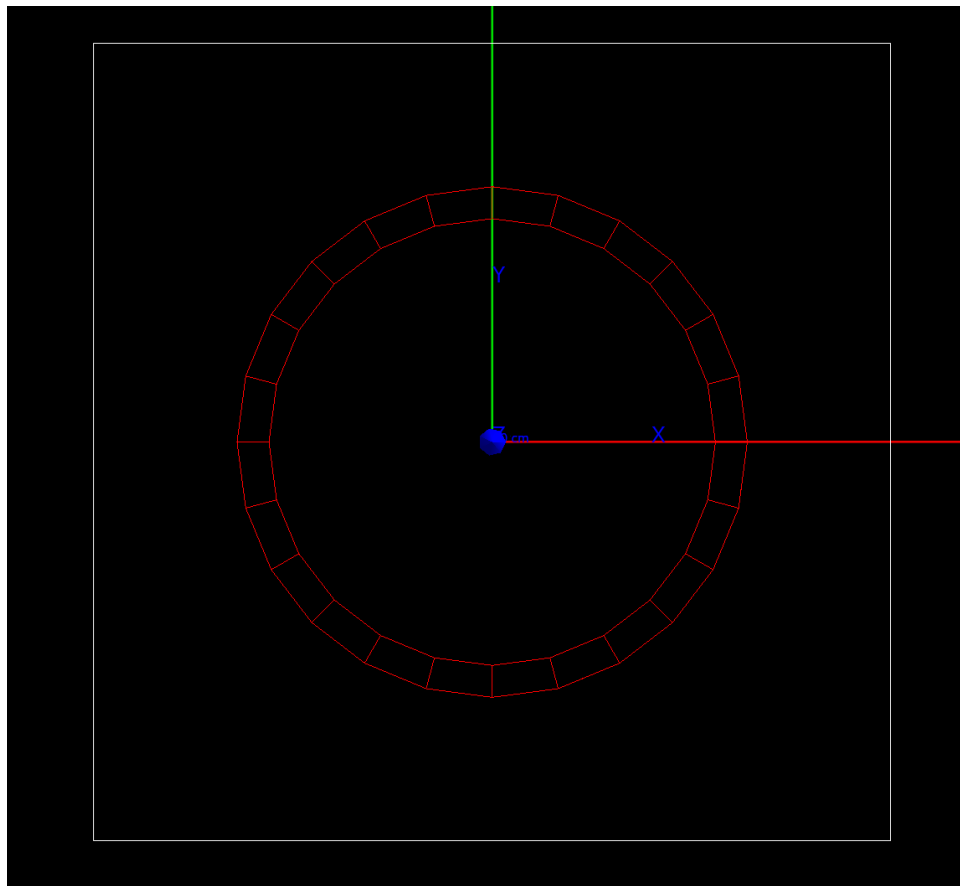


Figure 5: Side View of Base

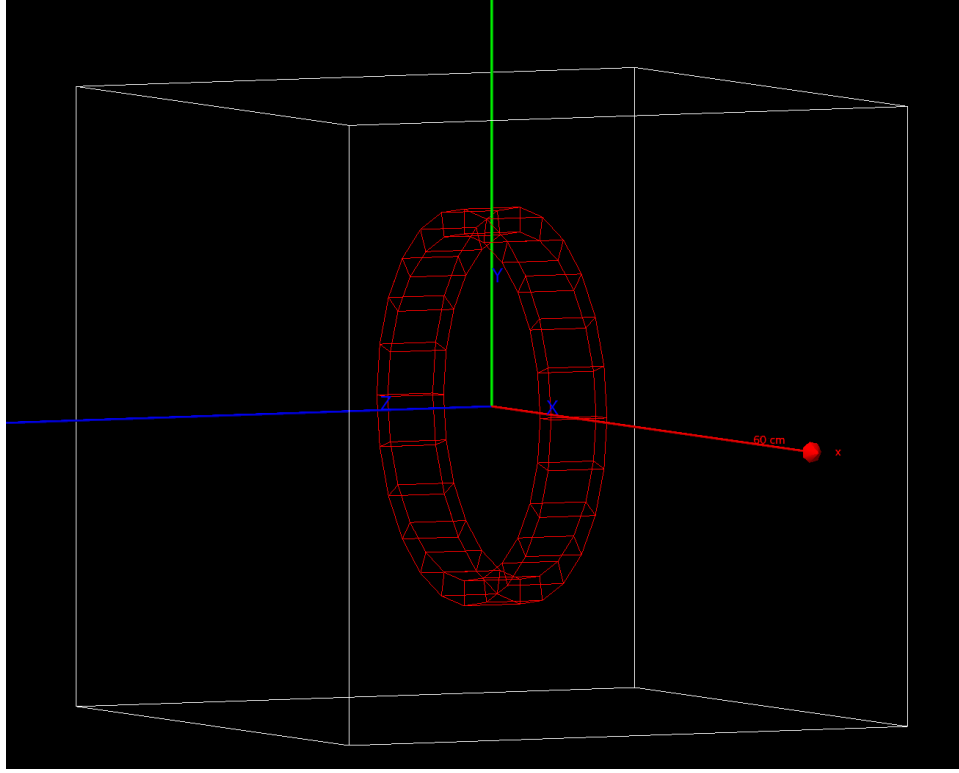


Figure 6: Angled View of Base

The second level of this volume is the Block which holds the  $48 \times 48$  array of LYSO crystals. The Block has a length and width of 4.8 cm and a thickness of 1.0 cm. Inside the Block, the single crystal's dimensions are defined: a length and width of 0.925 mm and 10 mm thick. The length and width are not exactly 1.0 mm because the physical crystals have a 0.075 mm gap filled with an adhesive to ensure no crosstalk occurs between neighbouring crystals. This one crystal is repeated throughout the space inside the Block 48 times to create the array. Figures 7 & 8 are illustrations of the Block and a close-up view of the the LYSO crystal matrix in the OGLIQt GUI.

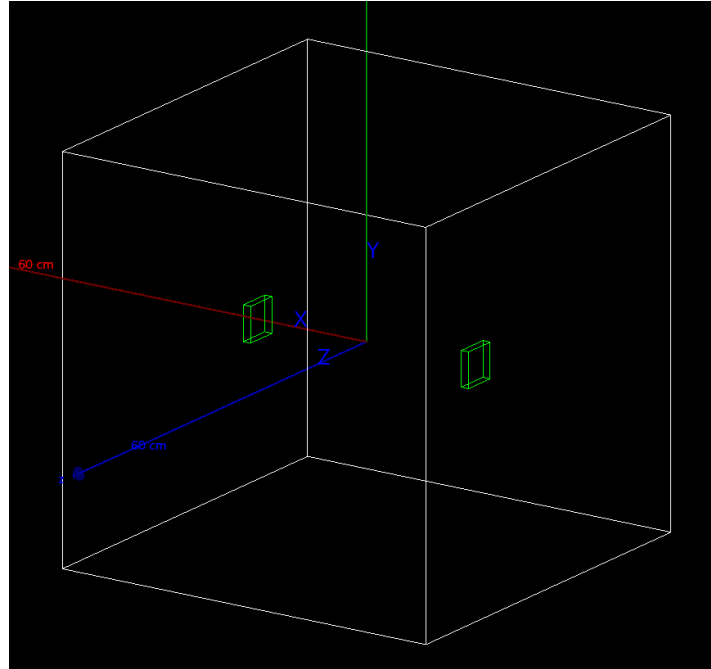


Figure 7: Block Setup

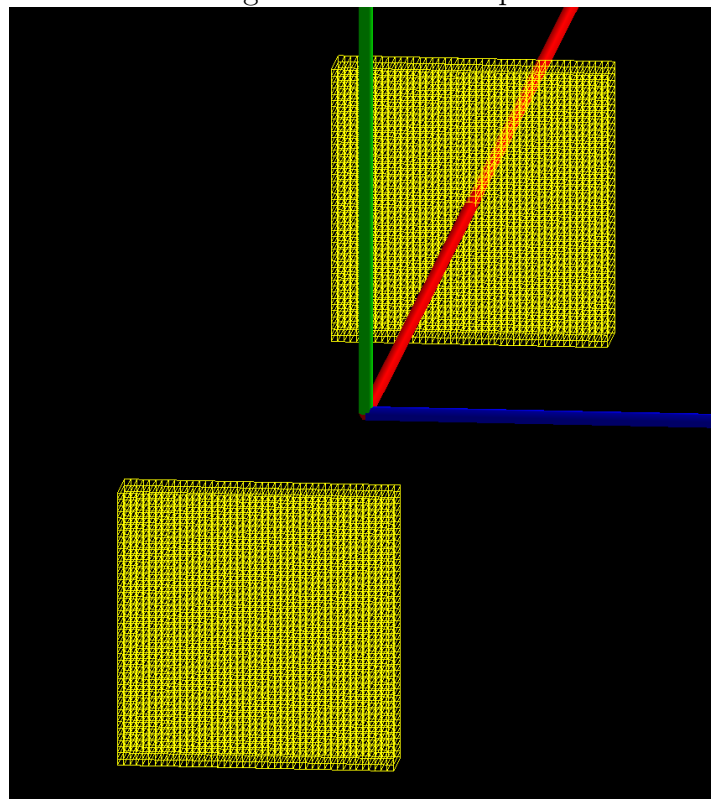


Figure 8: Crystal Setup

The Block was be repeated twice to set two Blocks facing one another within the cylindrical Base  $180^\circ$  from one another. For future simulations, these Blocks can be repeated more times and set at different angles from one another with the same LYSO crystal matrix. Figure 9 shows the complete geometry of this set up before adding a source.

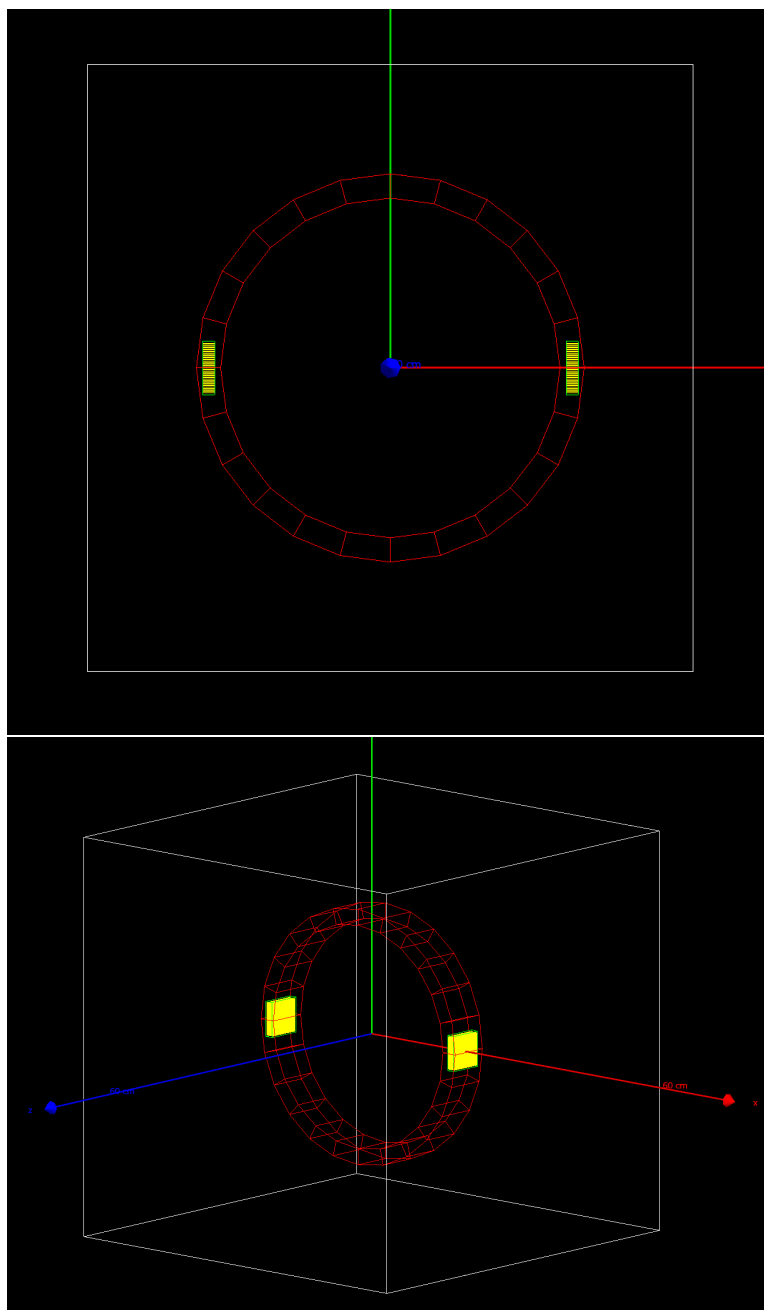


Figure 9: Side and Angles View of complete Geometry Setup



## source\_2gammasRDG.mac

In this macro, a point source is created which emits 2  $\gamma$ -rays, each with an energy of 0.511 MeV. The pair is emitted at exactly  $180^\circ$  from one another. There is an option to restrict the angles at which the source emits radiation. To save simulation time and only create coincident pairs of events, the source was restricted in the  $\theta$  and  $\phi$  angles accordingly.

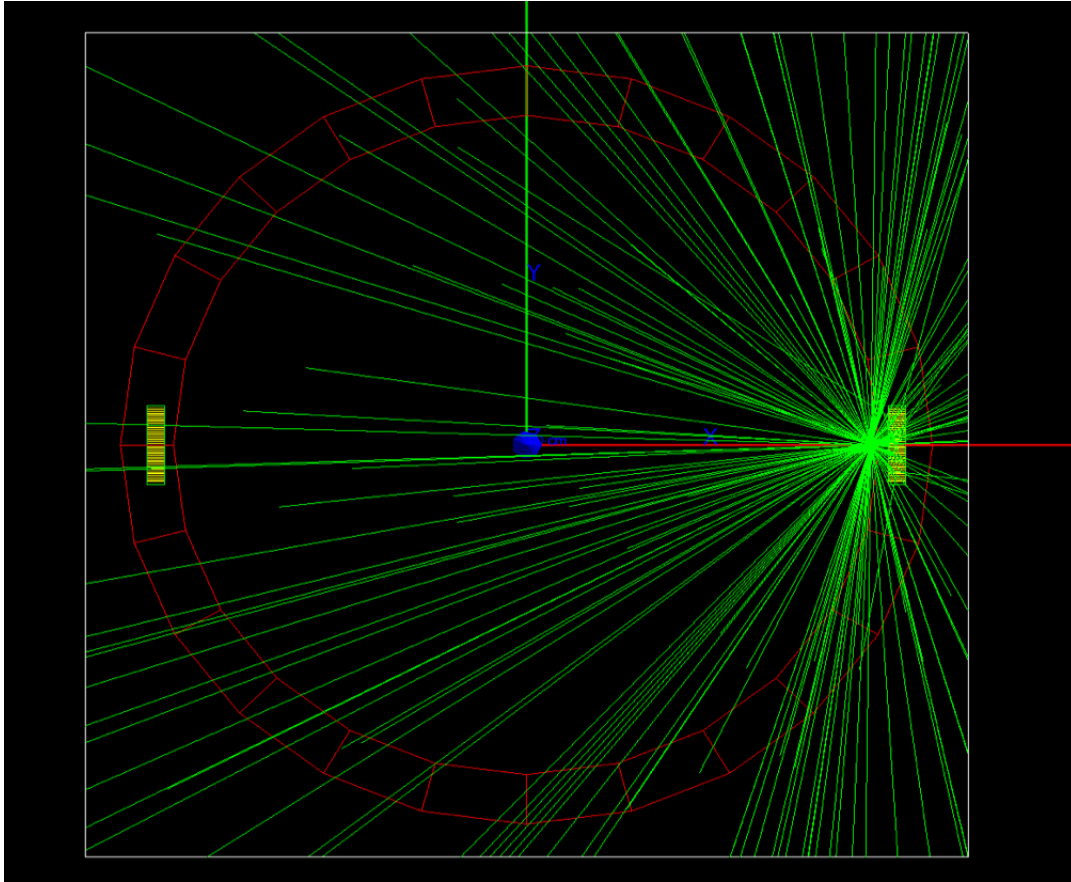


Figure 10: Unrestricted Source positioned closer to Detector B

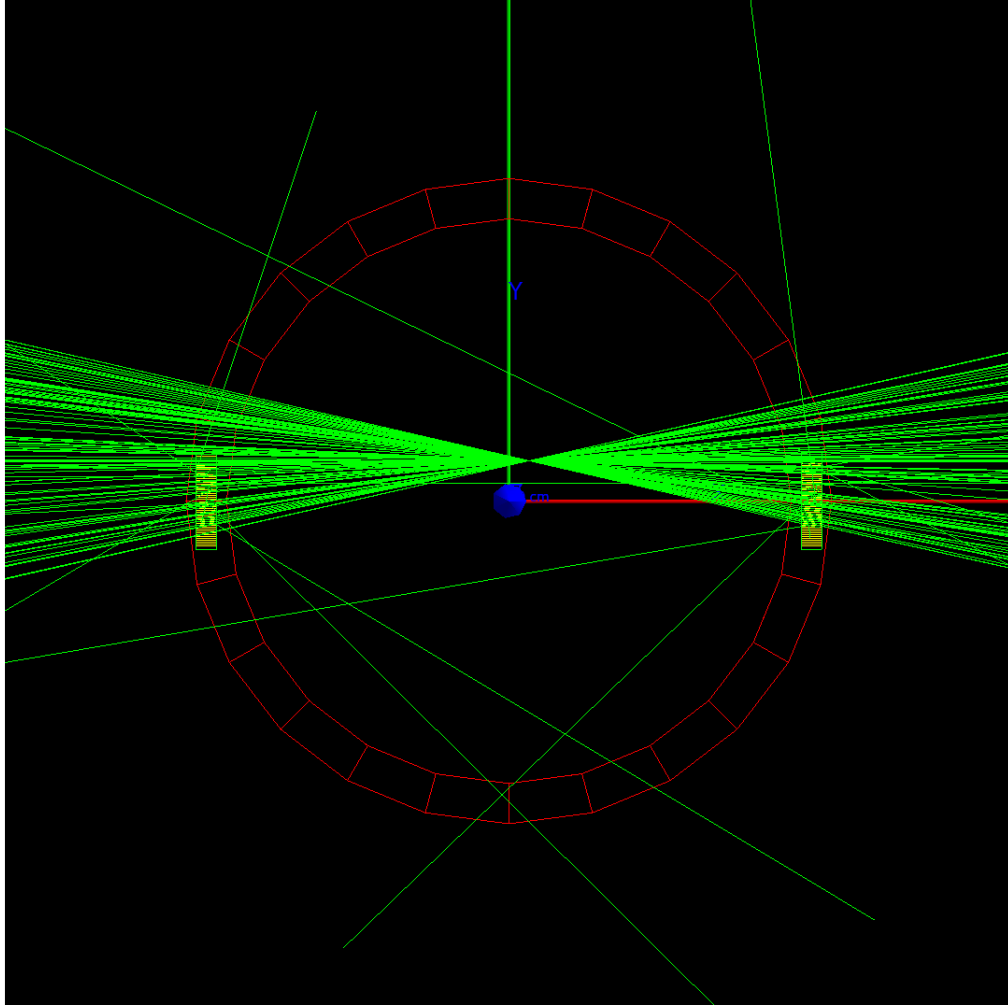


Figure 11: Restricted Source, Biased in All Three Axes

## physicsRDG.mac

This macro is where physical processes are added that mimic what occurs in the physical experiment. There is an option in GATE to simulate isotopes that decay, emit positrons, and then create an annihilation event with an electron. In this macro, the type of source used (either already emitting  $\gamma$ -rays or allowing an element to radioactively decay) determines what type of physical process is set in this macro. To use Fluorine-18, or another radioactive tracer, the process of ‘RadioactiveDecay’ would have to be enabled. This project’s

point source does not simulate the decay process, but immediately emits pairs of  $\gamma$ -rays. GATE's corresponding physical process is: 'emstandard\_opt1'. This means that standard electromagnetic processes are produced and a high energy parameterization model is used. Compton scattering, the photoelectric effect, gamma conversions etc. are defined for gamma rays, electrons, positrons, protons, muons, and antimuons with this parameter. There are five options of standard emission, each with different settings of precision and types of emission. 'emstandard\_opt1' is fast, but not as precise as the latter options 2-5. See [15] for more information about the different levels of standard physics processes.

## petDigiRDG.mac

GATE simulates what are called Hits. A Hit occurs when a particle interacts with matter. The position, time, momentum, interaction type, and energy deposition of the interaction are stored per Hit. Hit data is not representative of the data output observed from a PMT. This macro implements digitizer modules which mimic what a physical PMT produces. The output of each intermediate module is called a Pulse, with the final module in this series producing a Single (Figure 12).

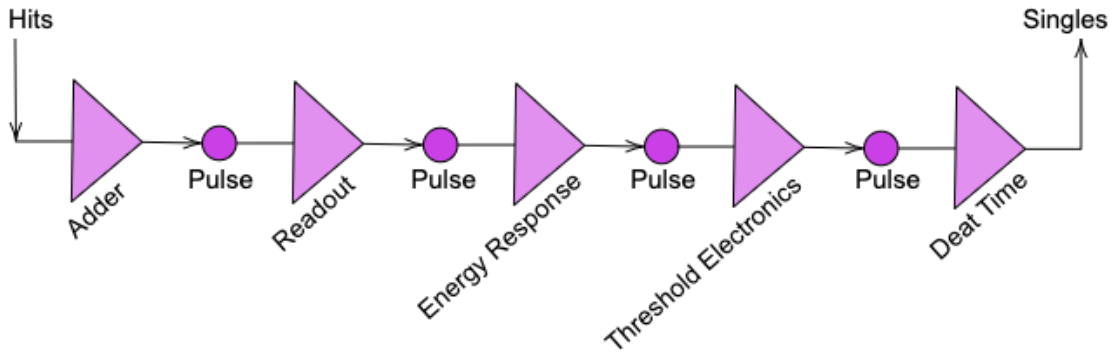


Figure 12: Flow Chart of Hits to Digitizer Modules to Singles

The Singles output file data was used to compare to observed data. Below are descriptions of each digitizer module incorporated into the simulation.

1. **Adder** This signal processing module adds up any hits that occur in the same crystal and calls this sum a Pulse.
2. **Readout** This module regroups the Pulses per Block. The level or depth options at which this occurs are based on the type of geometry system used. In the case of an Ecat system, there are two levels in which the readout can operate. Numbers correspond to the depth of the system. For example, `‘/gate/digitizer/Singles/readout/setDepth 1’` sets the regrouping to occur at the Block level. If the depth was set to two, it would only regroup hits at the crystal level. Adding at the Block level is more akin how the RDG’s detectors add events. The default setting for how this module regroups is via an ‘energy-centroid’ method. This collective module give a total energy per block. Figure 13 shows this process. For the purposes of this experiment, the last Pulse of the diagram below is what is defined as a Single.

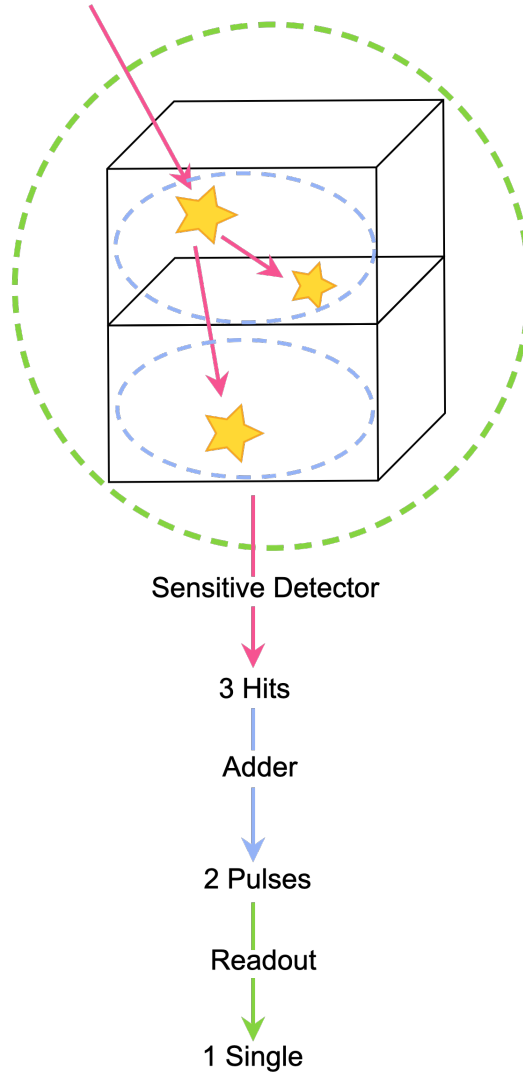


Figure 13: Flow Chart of Hits to a Single

3. **Energy Blurring** This module simulates the Gaussian blurring around a certain energy [16]. Working with the experimental data, the Full Width Half Maximum (FWHM) of the Gaussian produced around 511 keV was calculated. This was accomplished by finding the standard deviation,  $\sigma$ , of the experimental data and using the

approximation

$$FWHM = 2\sigma\sqrt{2\ln(2)} = 2.35\sigma$$

[17] to find the FWHM. The experimental data had a FWHM of 99.6 keV and peaked at 539 keV, this value was assumed to be the energy of reference. To use the inverse square law

$$R = \frac{R_0 E_0}{\sqrt{E}}$$

that GATE uses to create this energy blurr, a test simulation was run with the energy reference ( $E_0$ ) set to 511 keV and the energy resolution ( $R$ ) set to 0.13 to calculate the  $E$  value in the denominator (this value was not specified in the documentation).  $E$  was found to be equal to  $7.36 \times 10^{10}$ . This value was then used with the FWHM value and energy of reference from the experimental data and plugged into the inverse square law equation. The energy resolution of the experimental data was calculated to be 0.198. This was set to be the energy resolution in GATE, but with the energy of reference still set to 511 keV because the RDG shifts its data relative to forcing the Gaussian peak to line up at 511 keV in energy spectrum graphs.

4. **Thresholder/Upholder** This module sets an upper-bound and a lower-bound of energy to create an energy window, where any photons outside the set limits are disregarded. The window was set between 10 keV and 1000 keV.

## outputRDG.mac

In the output macro, .root and .txt output files are created and saved in an output folder. The .txt file saves information such as number of events, physical processes, elapsed time, simulation time, and start/end date. See Appendix B for an .txt file example. The .root files saves: raw Hit information, Singles, Coincidences, and Delays. To save memory and

the keep the size of these .root files to a minimum, it is possible to enable and disable what information will be saved. This project primarily used Singles data and not Hit data, so the Hit information was disabled.

## Data

Jupyter Notebooks, a web-application, was used to allow Python3 Libraries to analyze .root files. Using the Python library Uproot, the information GATE gave in a .root file was translated to Numpy arrays. The data was split up to each detector. Any event with a negative x-axis value meant it corresponded to one detector vs the other with a positive x-axis value. Below is a side view of the detectors and a scatter plot of the position of hits in the X-Y plane:

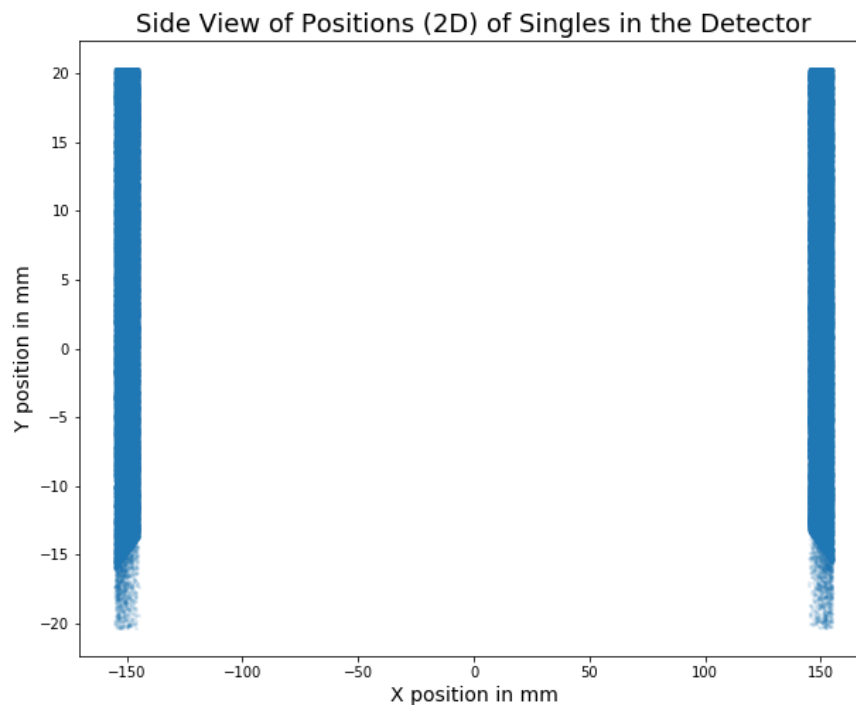


Figure 14: Side View Scatter Plot of Simulated Events

Histograms which count the number of Singles per crystal were created. Figure 15 and 16 are the  $44 \times 44$  bins showing how many Singles each individual crystal received for each detector. Figure 15 shows the RDG's data and Figure 16 shows the simulated data.

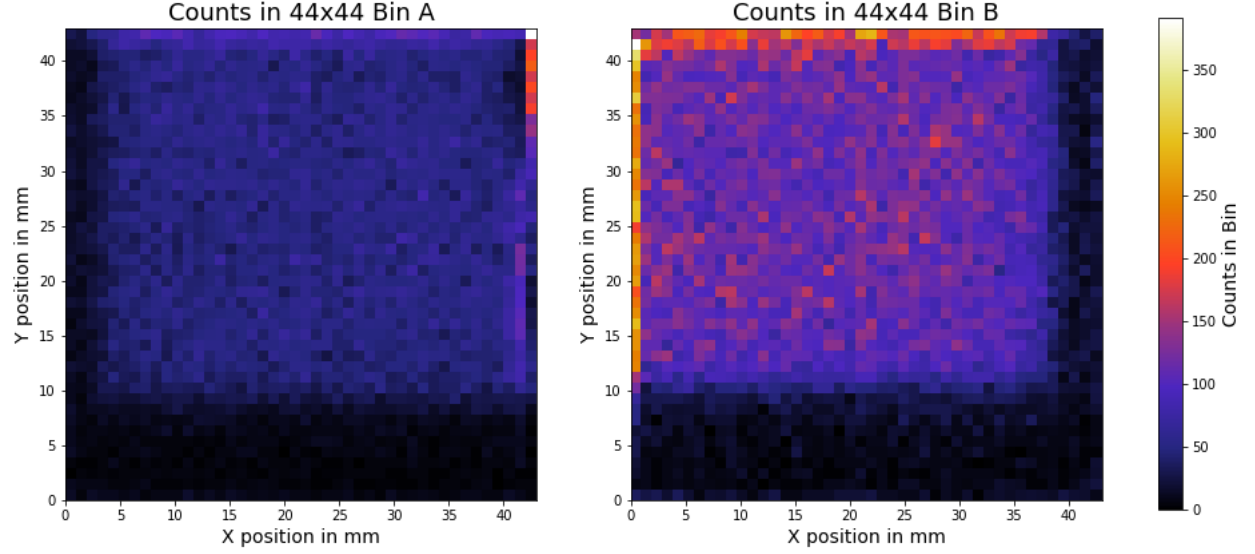


Figure 15: Number of Singles per Crystal Experimental Data

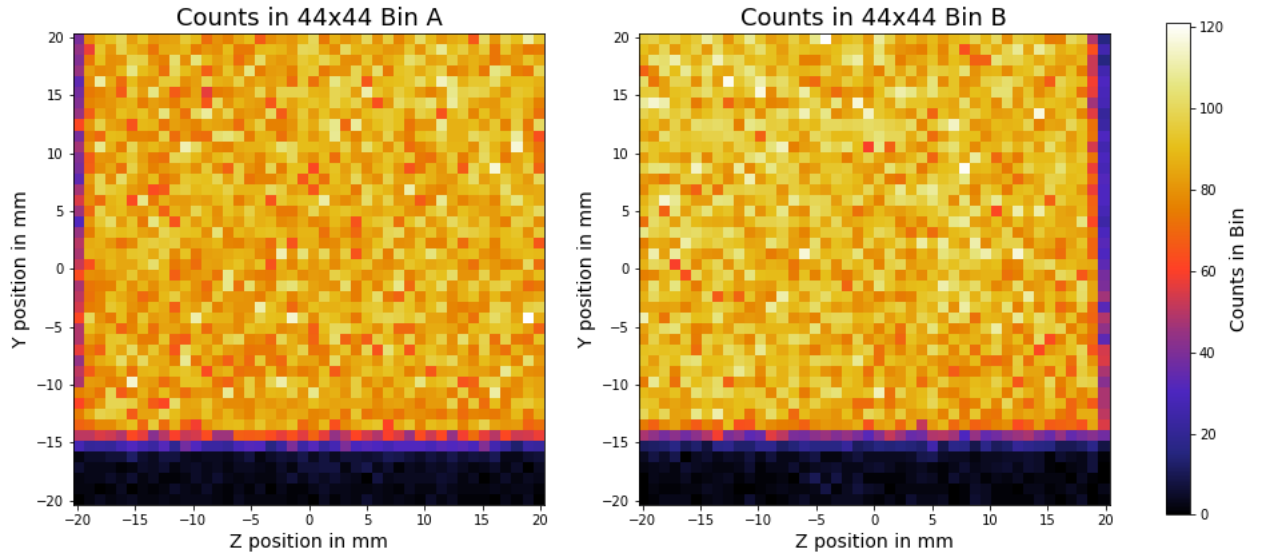


Figure 16: Number of Singles per Crystal Simulated Data



Due to edge cases in the experimental data, the data was cropped by 4 crystals inward. That is why there is only a matrix of  $44 \times 44$  crystals for this data comparison. The shadows in the experimental data are also shown in the simulated data. This supports the fact that GATE's point source can be placed in such a way that the same images that the RDG renders from a biased source in x, y, and z axes are produced. The experimental data had 161007 events and the simulated data to was cropped to only graph the first 161007 events to match.

The The RDG detectors have an  $8 \times 8$  anode output. The two graphs below show the experimental data and simulated data binned in  $8 \times 8$  blocks to depict what the PSPMT data produces.

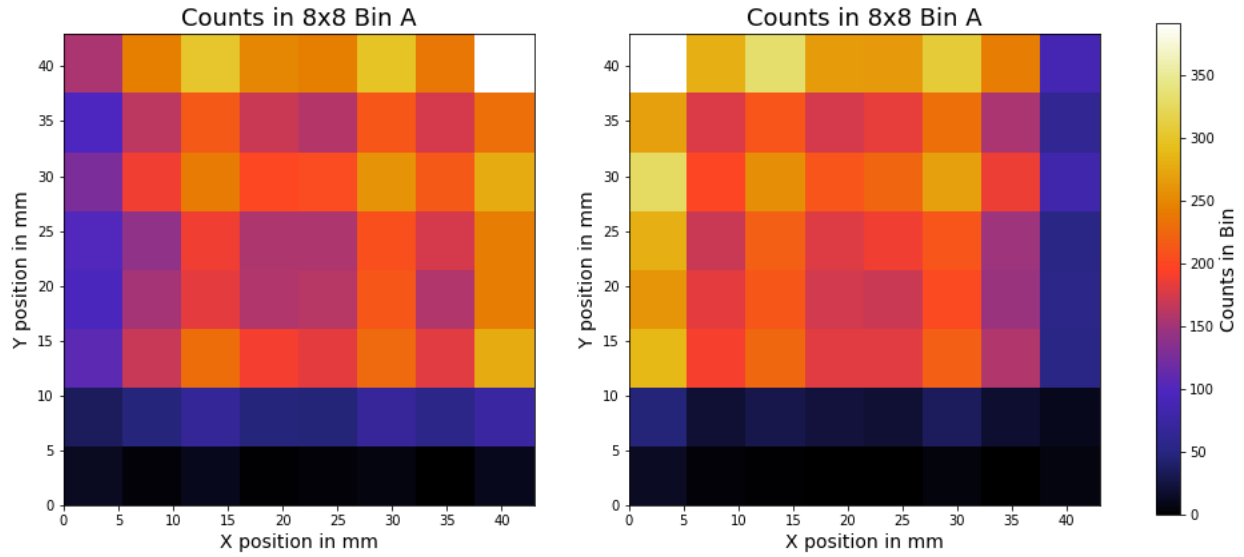


Figure 17: Number of Singles per Anode Experimental Data

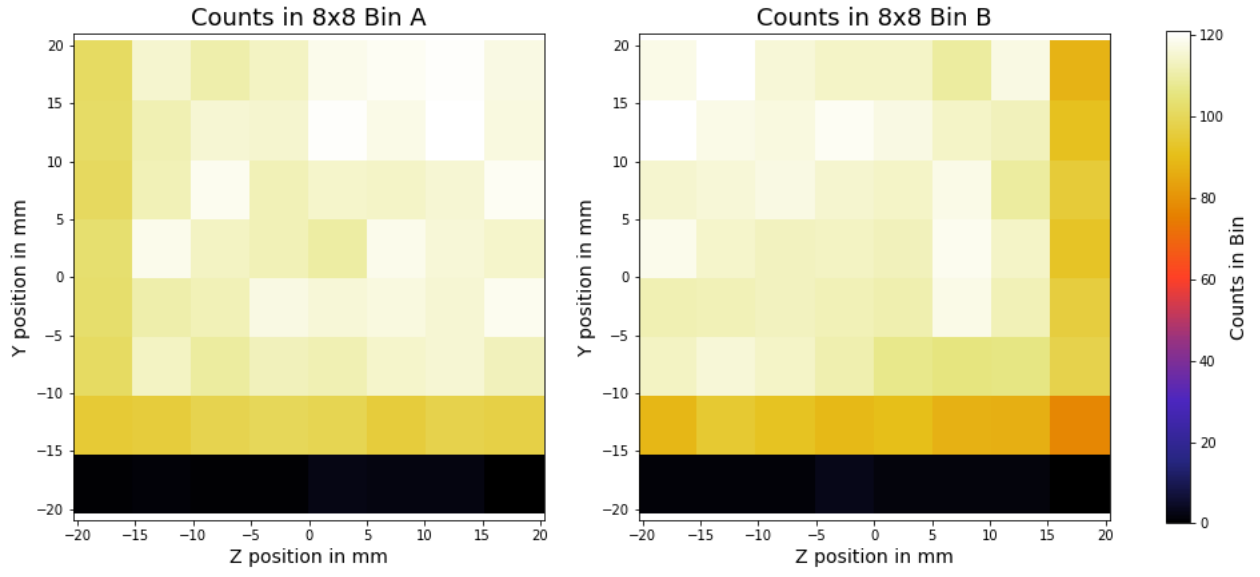


Figure 18: Number of Singles per Anode Simulated Data

Figures 19 and 20 are histograms of the energies deposited in the crystals.

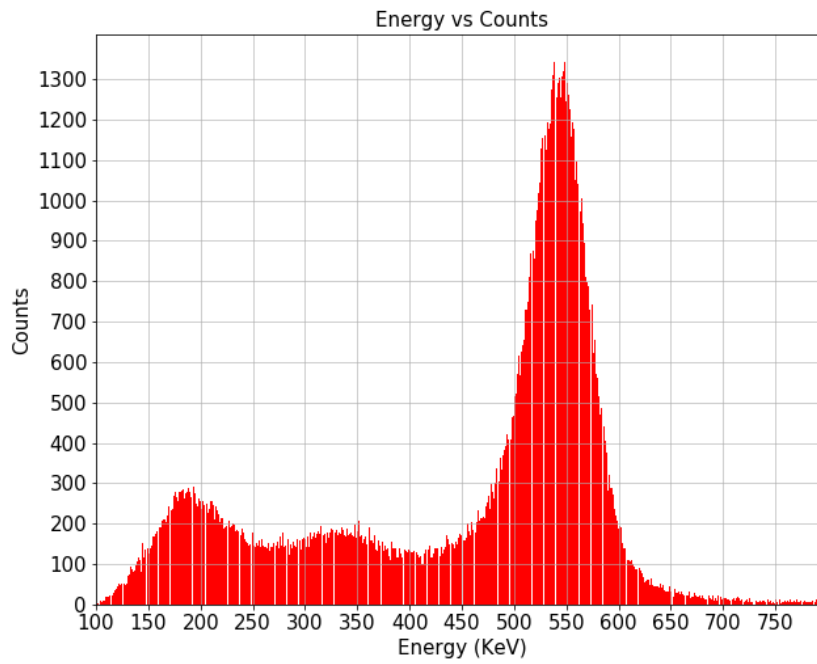


Figure 19: Energy Spectrum of Experimental data

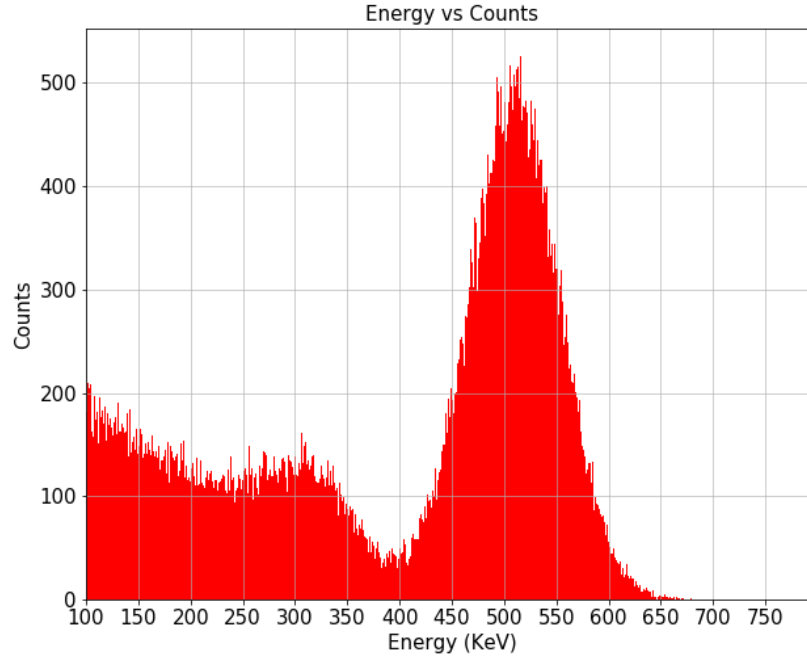


Figure 20: Energy Spectrum of Simulated Data

The experimental data had FWHM of 99.66 keV between 400 keV and 625 keV. The simulated data had a FWHM of 99.40 between 400 keV and 625 keV with the data cut off to match the number of events the of the experimental data. The experimental data has a mean of  $\approx 531$  keV and the simulated data peaked at  $\approx 509$  keV. The slightly higher mean value is expected for the experimental data (see point source macro for more information). The extra peak at about 175 keV that tails to 0 keV is from the way thresholds and coincident events are counted through the RDG's ADC channels. The extra data between 400 keV and 450 keV is due to noise in the phytoPET system. The peak around 307 keV is expected from the background radiation of Lutetium in the LYSO crystal.

## Discussion

Due to current restrictions to access JLab's facilities, the RDG was unable to take more comparable data. In future, Figure 21 can be supported and compared with future RDG research. The RDG saw these plots and noted that, graphically, this is what would be expected from a point source that was biased in only the x-axis.

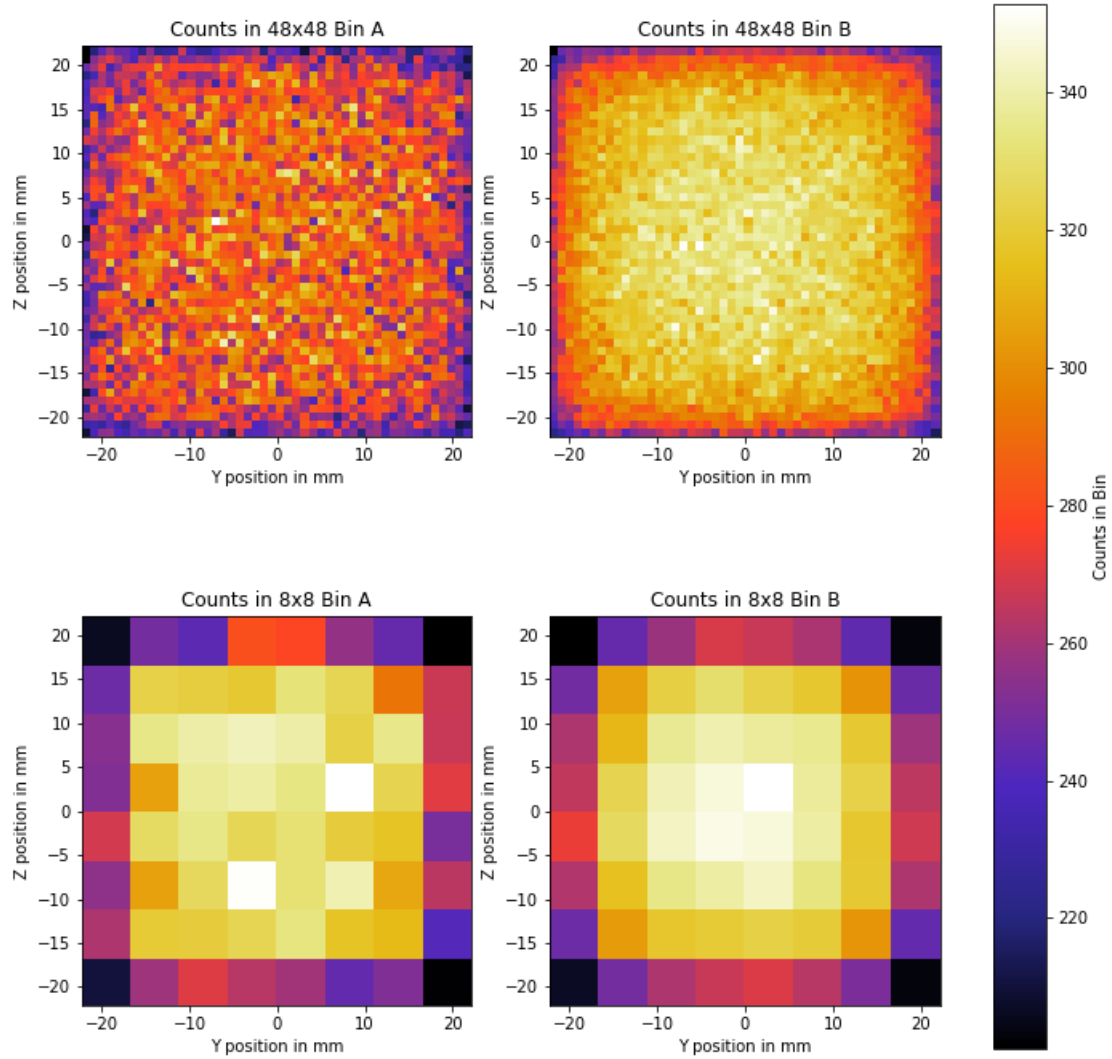


Figure 21: Number of Singles per Crystal (top) and Anode (Bottom) for Simulated Data

GATE also can have various shaped sources of radiation, such as a cylinder. This could be used instead of a point source to mimic the image of a plant stem in further research.

Overall, comparing the simulated and experimental data, GATE has been validated as functioning properly. This project determined GATE a suitable tool for the RDG to employ in their research and design of future detector systems. The GATE macros and Python program written will be a software template which the RDG can use to model further components of their detector system.

# Appendix

## Appendix A: mainRDG.mac

```
# Visualisation
/control/execute phytoPet/visuRDG.mac

# Verbosity
/control/execute phytoPet/verboseRDG.mac

# Geometry
/control/execute phytoPet/worldRDG.mac
/control/execute phytoPet/geoRDG.mac
/control/execute phytoPet/petDigiRDG.mac
#/control/execute phytoPet/cylindrical_phantom.mac

# Physics
/control/execute phytoPet/physicsRDG.mac

# Output
/control/execute phytoPet/outputRDG.mac

# Initialisation
/gate/run/initialize

# Source
#/control/execute phytoPet/source_f18.mac
/control/execute phytoPet/source_2gammasRDG.mac

# Random
/gate/random/setEngineName MersenneTwister
/gate/random/setEngineSeed auto

# Start acquisition
/gate/application/setTimeStart 0 s
/gate/application/setTimeSlice 1500 s
/gate/application/setTimeStop 1500 s
/gate/application/start
```

## Appendix B: .txt Output File Example

```
# NumberOfRun = 1
# NumberOfEvents = 299959
# NumberOfTracks = 724230
# NumberOfSteps = 4994082
# NumberOfGeometricalSteps = 3991944
# NumberOfPhysicalSteps = 1002138
# ElapsedTime = 31.3491
# ElapsedTimeWoInit = 30.5557
# StartDate = Wed Apr 8 13:45:07 2020
# EndDate = Wed Apr 8 13:45:38 2020
# StartSimulationTime = 0
# StopSimulationTime = 300
# CurrentSimulationTime = 300.001
# VirtualStartSimulationTime = 0
# VirtualStopSimulationTime = 300
# ElapsedSimulationTime = 300.001
# PPS (Primary per sec) = 9816.81
# TPS (Track per sec) = 23702
# SPS (Step per sec) = 163442
```

## Appendix C: petDigiRDG.mac

```
# The singles

/gate/digitizer/Singles/insert          adderCompton
/gate/digitizer/Singles/insert          adder
/gate/digitizer/Singles/insert          readout
/gate/digitizer/Singles/readout/setDepth 1
/gate/digitizer/Singles/insert          blurring
/gate/digitizer/Singles/blurring/setResolution 0.198
/gate/digitizer/Singles/blurring/setEnergyOfReference 511. keV
/gate/digitizer/Singles/insert          thresholder
/gate/digitizer/Singles/thresholder/setThreshold 0 keV
/gate/digitizer/Singles/insert          upholder
/gate/digitizer/Singles/upholder/setUphold 1 MeV

# ATTACHEMENT TO THE SYSTEM

#/gate/systems/system_name/system_level_name/attach
volume_name

#..
#..

# Deadtime

# the deadtime is applied on the "blockDetector" defined in geoRDG.mac

# /gate/digitizer/Singles/insert          deadtime
# /gate/digitizer/Singles/deadtime/setDeadTime 3000 ns
# /gate/digitizer/Singles/deadtime/setMode nonparalysable
#/gate/digitizer/Singles/deadtime/chooseDTVVolume blockDetector
# /gate/digitizer/Singles/deadtime/chooseDTVVolume ecat
#/gate/digitizer/Singles/deadtime/chooseDTVVolume crystalUnit
# /gate/digitizer/Singles/deadtime/setBufferSize 1 MB
# /gate/digitizer/Singles/deadtime/setBufferMode 0
```



```

# Coincidence sorter
# Define a delay coincidence sorter
# To estimate random coincidences

/gate/digitizer/Coincidences/setWindow      10 ps
/gate/digitizer/Coincidences/MultiplesPolicy takeWinnerIfIsGood
#/gate/digitizer/Coincidences/MultiplesPolicy takeWinnerOfGoods
#/gate/digitizer/name                       delay
#/gate/digitizer/insert                     coincidenceSorter
#/gate/digitizer/delay/setWindow            5 ns
#/gate/digitizer/delay/setOffset            0.001 ns
#/gate/digitizer/delay/MultiplesPolicy      takeWinnerIfIsGood
#/gate/digitizer/delay/MultiplesPolicy      takeWinnerOfGoods

```

## References

- [1] Weisenberger, A., Dong, H., Kross, B., Lee, S., Mckisson, J., Mckisson, J., ... Stolin, A. (2011). Development of PhytoPET: A plant imaging PET system. *2011 IEEE Nuclear Science Symposium Conference Record*, 275–278. doi: 10.1109/nssmic.2011.6154496
- [2] GATE: Simulations of Preclinical and Clinical Scans in Emission Tomography, Trans-mission Tomography and Radiation Therapy. (n.d.). Retrieved October 1, 2019, from <http://www.opengatecollaboration.org/home>. Saint-Gobain Ceramics Plastics, Inc. (2018).
- [3] Thornton, S. T., & Rex, A. (2013). *Modern Physics: For Scientists and Engineers*. Boston: Brooks/Cole.
- [4] *PET Imaging Illustration*. (2019, January 29). Retrieved from <https://www.radiologycafe.com/images/physics/nm-pet-lineofresponse@2x.png>
- [5] Weisenberger, A. G., Kross, B., Lee, S., Mckisson, J., Mckisson, J. E., Xi, W., ... Smith, M. F. (2012). PhytoBeta imager: a positron imager for plant biology. *Physics in Medicine and Biology*, 57(13), 4195–4210. doi: 10.1088/0031-9155/57/13/4195
- [6] Hamamastu Photonics. (2011). *Flat Panel Type Multianode Pmt Assembly H8500 Series/H10966 Series*. Retrieved from [https://www.hamamatsu.com/resources/pdf/etd/H8500\\_H10966\\_TPMH1327E.pdf](https://www.hamamatsu.com/resources/pdf/etd/H8500_H10966_TPMH1327E.pdf).
- [7] Melcher, C. L. (2000). Scintillation Crystals for PET\*. *Journal of Nuclear Medicine*, (41), 1051–1055. Retrieved from <http://jnm.snmjournals.org/content/41/6/1051.full.pdf>
- [8] Hamamastu Photonics. (2007). *Photomultiplier Tubes: Basics and Applications*. (3rd ed.). Retrieved from [https://www.hamamatsu.com/resources/pdf/etd/PMT\\_handbook\\_v3aE.pdf](https://www.hamamatsu.com/resources/pdf/etd/PMT_handbook_v3aE.pdf)

- [9] Popov, V., Majewski, S., & Weisenberger, A. (2003). Readout electronics for multi-anode photomultiplier tubes with pad matrix anode layout. *2003 IEEE Nuclear Science Symposium. Conference Record (IEEE Cat. No.03CH37515)*. doi: 10.1109/nssmic.2003.1352307
- [10] *Photomultiplier Tube Diagram*. (2007). Retrieved from [https://www.hamamatsu.com/resources/pdf/etd/PMT\\_handbook\\_v3aE.pdf](https://www.hamamatsu.com/resources/pdf/etd/PMT_handbook_v3aE.pdf)
- [11] Dubois, A., Sarrut, D. (2017, April 3). *OpenGATE/GATEContrib*. Retrieved October 17, 2019, from <https://github.com/OpenGATE/GATEContrib/tree/master/imaging/PET>.
- [12] Sarrut, D. (2019, April). *gate-exercices/pet*. Retrieved from <https://gitlab.in2p3.fr/davidsarrut/gate-exercices/tree/master/pet/mac>.
- [13] Mao, R., Zhang, L., Zhu, R. (2007). Optical and Scintillation Properties of Inorganic Scintillators in High Energy Physics. *2007 IEEE Nuclear Science Symposium Conference Record*, 2285-2291. doi: 10.1109/NSSMIC.2007.4436602
- [14] Lowdon, M., Martin, P. G., Hubbard, M., Taggart, M., Connor, D. T., Verbelen, Y., ... Scott, T. B. (2019). Evaluation of Scintillator Detection Materials for Application within Airborne Environmental Radiation Monitoring. *Sensors*, 19(18), 3828. doi: 10.3390/s19183828
- [15] Geant4 Collaboration. (2018). Tables by constructor. Retrieved April 17, 2020, from [http://geant4-userdoc.web.cern.ch/geant4-userdoc/UsersGuides/PhysicsListGuide/html/electromagnetic/tables\\_by\\_constructor/index.html](http://geant4-userdoc.web.cern.ch/geant4-userdoc/UsersGuides/PhysicsListGuide/html/electromagnetic/tables_by_constructor/index.html)
- [16] GATE Documentation. (2019, October 9). Retrieved October 13, 2019, from <https://opengate.readthedocs.io/en/latest/#welcome-to-gate-s-documentation>.

- [17] Leo, W. R. (1994). Statistics and the Treatment of Experimental Data. In Techniques for nuclear and particle physics experiments a how-to approach. Retrieved from [https://ned.ipac.caltech.edu/level5/Leo/Stats\\_contents.html](https://ned.ipac.caltech.edu/level5/Leo/Stats_contents.html)
- [18] Lazaro, D., Buvat, I., Loudos, G., Strul, D., Santin, G., Giokaris, N., ... Breton, V. (2004). Validation of the GATE Monte Carlo simulation platform for modelling a CsI(Tl) scintillation camera dedicated to small-animal imaging. *Physics in Medicine and Biology*, 49(2), 271–285. doi: 10.1088/0031-9155/49/2/007